Effect of Modification with Vanadium or Carbon on Destructive Sorption of Halocarbons over Nanocrystalline MgO: The Role of Active Sites in Initiation of the Solid−State Reaction

ARTICLE *in* THE JOURNAL OF PHYSICAL CHEMISTRY C · JUNE 2014

Impact Factor: 4.77 · DOI: 10.1021/jp503916e

9 AUTHORS, INCLUDING:

Alexander Volodin
Boreskov Institute of Catalysis
99 PUBLICATIONS **1,438** CITATIONS
SEE PROFILE

Ilya V Mishakov
Boreskov Institute of Catalysis
56 PUBLICATIONS **366** CITATIONS
SEE PROFILE

Aleksey Vedyagin
Boreskov Institute of Catalysis
50 PUBLICATIONS **151** CITATIONS
SEE PROFILE

V. V. Chesnokov
Boreskov Institute of Catalysis
63 PUBLICATIONS **679** CITATIONS
SEE PROFILE

THE JOURNAL OF PHYSICAL CHEMISTRY C

Article

pubs.acs.org/JPCC

Effect of Modification with Vanadium or Carbon on Destructive Sorption of Halocarbons over Nanocrystalline MgO: The Role of Active Sites in Initiation of the Solid-State Reaction

Alexander F. Bedilo,*[,†,‡] Ekaterina I. Shuvarakova,[†,‡] Alexander M. Volodin,[†] Ekaterina V. Ilyina,[†] Ilya V. Mishakov,[†,§] Aleksey A. Vedyagin,[†,§] Vladimir V. Chesnokov,[†,§] David S. Heroux,[∥] and Kenneth J. Klabunde[⊥]

[†]Boreskov Institute of Catalysis SB RAS, Prospekt Lavrentieva 5, Novosibirsk 630090, Russia

[‡]Novosibirsk Institute of Technology, Moscow State University of Design and Technology, Krasny Prospekt 35, Novosibirsk 630099, Russia

[§]Novosibirsk State Technical University, Prospekt Karla Marksa 20, Novosibirsk 630092, Russia

[∥]Department of Chemistry and Physics, Saint Michael's College, Colchester, VT 05439, United States

[⊥]Department of Chemistry, Kansas State University, Manhattan, Kansas 66506, United States

ABSTRACT: Small amounts of vanadium or carbon added to nanocrystalline MgO aerogels were shown to promote their activity in destructive sorption of CF_2Cl_2 and $CFCl_3$ halocarbons. This reaction is characterized by a prolonged induction period, which is considerably shortened after the addition of the studied promoters. It was demonstrated that the promoting effect of finely dispersed carbon did not depend on its location relative to the MgO nanoparticles. Approximately the same results were obtained when carbon was deposited as a thin layer on the surface of the MgO nanoparticles, when activated carbon was physically mixed with the nanocrystalline MgO or when it was located separately in the reactor. The modifying agents are believed to have a catalytic effect on the reaction of nanocrystalline MgO with halocarbons, accelerating the formation of active sites on the surface of the MgO nanoparticles. Electron-acceptor sites are shown to be possible candidates for the role of such active sites. The concentration of weak electron-acceptor sites tested by electron paramagnetic resonance (EPR) using anthracene as a spin probe increases during the induction period, reaching a well-defined maximum during the active stage of the reaction. Electron-acceptor sites of medium strength characterized by direct ionization of anthracene after adsorption were observed on the surface only during the active stage of the reaction. The studied reaction appears to be one of the first solid-state reactions where the role of surface active sites has been identified.

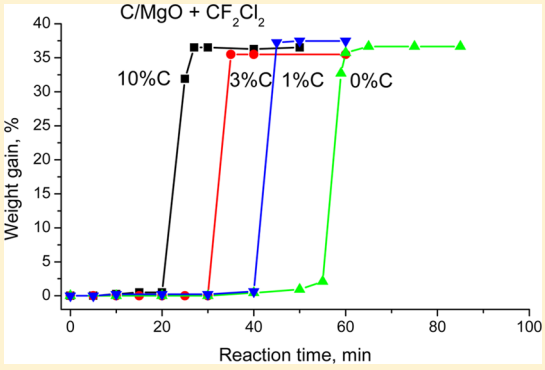

INTRODUCTION

The properties of nanoparticles are known to be sometimes quite different from those of bulk materials. For instance, the reactivity of metal oxides substantially increases when the dimensions of their particles is decreased down to several nanometers due to the increased ratio of their surface area to the bulk volume and high concentration of various active sites on the surface. Particularly remarkable in this respect are nanocrystalline mesoporous aerogels of alkaline earth metal oxides, which have been reported to possess high surface areas and outstanding reactivity with respect to variety of harmful organic substances.[1−4] At room temperature, these materials are capable of adsorbing acid gases and destroying spores and bacteria.[3,5,6] At elevated temperatures nanocrystalline metal oxide aerogels can be used as destructive sorbents for detoxification of halogenated and organophosphorus compounds and as catalysts or catalyst supports.[2,7−20]

Halocarbons, especially the ones containing no hydrogen atoms, are extremely stable and contribute to the destruction of the Earth's ozone layer. Therefore, development of active destructive sorbents capable of their decomposition without harming the environment is of substantial practical interest. Earlier we reported that nanocrystalline MgO aerogels react with CF_2Cl_2 starting from 325 °C, and this reaction is characterized by an unusual long induction period.[16,20] As the surface area of the nanocrystalline sorbent is very high and only decreases during the induction period, the beginning of the active phase must be due to the formation of some new active sites. Their origin was not understood until now.

Received: April 22, 2014
Revised: June 10, 2014
Published: June 10, 2014

Electron-donor and electron-acceptor sites detected by electron paramagnetic resonance (EPR) using suitable spin probes are well-known in the literature.[21−25] This approach is based on the use of specific molecules (probes) that selectively interact with the surface sites yielding surface paramagnetic species observed by EPR. Such sites capable of generating radical ion species after adsorption of donor or acceptor molecules are very active at least in these reactions.

Aromatic nitro compounds are most frequently used as the probe molecules for investigation of the electron-donor sites due to their pronounced electron acceptor properties and formation of relatively stable radical anions. Such sites were discovered on the surface of several typical oxide supports, such as Al_2O_3, MgO, ZrO_2, etc.[25−29] Recent data suggest that such sites might account for stabilization of finely dispersed palladium species, which are active in CO oxidation at low temperatures.[30]

Electron-acceptor sites are capable of generating radical cations by abstracting an electron from aromatic donor molecules.[21] This process results in the formation of radical cations that can either be observed by EPR directly[21,31−33] or can participate in reactions leading to the formation of secondary paramagnetic products on the surface.[21,34−36] The strength of the surface acceptor sites can be qualitatively characterized by the donor properties of the molecules that can be ionized on such sites. Recently we reported an excellent correlation between the concentrations of weak electron-acceptor sites observed after anthracene adsorption followed by heating at 80 °C and the catalytic activity of doped alumina catalysts in ethanol dehydration.[37]

Introduction of transition metal promoters was reported to increase the activity of MgO and CaO in destructive sorption of chlorinated compounds, vanadium being the most active promoter.[2] The MgO modification with vanadium was also found to increase its reactivity in reaction with $CFCl_3$ and CF_2Cl_2.[13,38,39] Carbon is another additive known to improve the destructive sorption properties of the MgO aerogels.[1,26,40] The introduction of a permeable carbon coating was reported to improve the stability of MgO aerogels in the presence of atmospheric moisture while preserving their reactivity in destructive sorption of halogenated compounds. The effect of the carbon coating on the MgO reaction with halocarbons has not yet been studied.

In the current study we investigated how vanadium added by mechanical mixing of the MgO aerogels with ammonium vanadate followed by calcination affects destructive sorption of CF_2Cl_2. We also studied the effect of finely dispersed carbon on this reaction. For both systems it was shown that the modifying agents can catalytically accelerate the solid-state reaction of the MgO aerogels with the halocarbons, apparently, by forming intermediates creating active sites on the MgO surface. Changes in the concentrations of surface electron-donor and electron acceptor sites during the reaction of the MgO aerogel with CF_2Cl_2 were studied for the first time. The obtained results suggest that weak electron-acceptor sites formed during the induction period may account for the active stage of the process.

EXPERIMENTAL SECTION

Two samples of nanocrystalline magnesium oxide synthesized by modified aerogel method (AP-MgO) were used in the study. The synthesis procedure included reaction of magnesium metal ribbon with methanol, addition of toluene as a second solvent, hydrolysis by a small amount of water to form a clear gel, drying in an autoclave under supercritical conditions, and heat-treatment under vacuum with gradual temperature increase to 500 °C as described in detail previously.[1,3,15] The surface areas of the studied samples differed by almost a factor of 2: 385 and 760 m^2/g. The samples were denoted as AP-MgO-1 and AP-MgO-2, respectively. As mentioned by us earlier, the specific surface area of the MgO aerogels substantially depends on minor details of the synthesis procedure, particularly calcination after the supercritical drying.[11]

A flow gas reactor equipped with a McBain spring balance was used for synthesis of the carbon coating on MgO surface "in situ" according to the method similar to the one reported earlier.[26] AP-MgO-1 was placed in a quartz basket hanging on a quartz spring. This method allowed us to control changes of the sample weight during reaction with 10^{-4} g precision and precisely determine the mass of deposited carbon. First, the samples were heated in an argon flow (75 l/h) for 1 h at 500 °C. Then, the gas was changed for 1,3-butadiene (7.5 l/h), which was used as the source of carbon. Carbon was formed on the AP-MgO surface with the initial rate of 2 wt %/h. After the desired carbon concentration was obtained, the butadiene flow was stopped, and the samples were cooled in the argon flow to room temperature.

V_2O_5/AP-MgO samples were prepared by grinding AP-MgO-2 with the desired amount of ammonium vanadate (Aldrich) in a ceramic mortar. Then, the samples were heated under vacuum at 450−600 °C for 2 h with gradual temperature increase. Under these conditions, ammonium vanadate first melted, filling the AP-MgO pores, and then decomposed to vanadium(V) oxide. After calcination, the sample was slowly cooled down to room temperature under continuous evacuation.

The decomposition of the halocarbons was studied in the flow reactor with a McBain spring balance equipped with an online gas chromatograph. The setup allowed us to continuously monitor the sample weight and occasionally study the gas-phase composition. Pure-grade CF_2Cl_2 and $CFCl_3$ and high purity argon were used in the experiments. The Ar purity was no less than 99.99% with oxygen concentration less than 0.001% and water content below 0.1 g/m^3. One hundred milligrams of the studied sample was placed into the basket. Unless specially mentioned, before reaction with the halocarbon, the sample was activated at 500 °C for 30 min. The halocarbons were passed thought the reactor with a rate of 3 l/h. After the end of the reaction, the sample was cooled under argon flow to room temperature.

Granulated activated carbon was used in the experiments on the effect of mechanical mixing with AP-MgO on the halocarbon decomposition. The carbon granules were ground into powder and mixed with the AP-MgO-1 sample in the desired ratio. We also studied the effect of layered loading when the AP-MgO layer was placed above or below the carbon layer in the basket without mixing. Finally, in some experiments the samples were placed completely apart in the basket of the McBain balance without direct contact of the MgO and carbon phases.

The X-ray diffraction (XRD) experiments were carried out using a URD-63 diffractometer with CuKα irradiation. The diffraction patterns were recorded in the 2θ range 10−90° with 0.05° step and 10 s accumulation in each point. The phase composition of the samples was analyzed using a PC PDF database. Precise parameters of the MgO lattice were

dx.doi.org/10.1021/jp503916e | J. Phys. Chem. C 2014, 118, 13715−13725

determined by the least-squares deviations method using positions of 5 diffraction peaks. The average crystallite sizes were determined by the Scherer formula using the half-width of the most intense peak (200) of the MgO phase. The analysis of the diffraction peak half-width dependence on the reflection angle showed the lack of noticeable microdistortions in the structure of all the studied MgO samples.

An ERS-221 EPR spectrometer working in the X-band (ν = 9.3 GHz) was used in the study. The EPR spectra were recorded at 20 dB attenuation with typical microwave power 3 mW. The frequency of the microwave irradiation and the magnetic field were measured using a ChZ-64 frequency meter and a Radiopan MJ-100 magnetometer, respectively. The experimental installation was described in more detail previously.[41] The spectrometer operation and the analysis of the obtained results were performed using a PC and the software package EPR-CAD developed in our laboratory. The concentrations of the paramagnetic species were determined by numerical double integration with baseline compensation. A DPPH standard was used for calibration. Rigid sample placement in the spectrometer resonator and computer processing of the spectra allowed us to decrease typical errors in the determination of the relative radical concentrations to ±10%.

The concentrations of electron-donor and electron-acceptor sites during the CF_2Cl_2 destructive sorption were measured using the following original procedure. A sample of AP-MgO-2 was loaded into an EPR sample tube, which was placed into a catalytic installation equipped with a furnace and gas flow meters. A thin metal tube used for feeding gases to the sample was placed inside the EPR tube. The exit from the metal tube was located at 5 mm from the surface of the sample. Preliminary experiments demonstrated that the sample was rather uniformly treated with the reactant, although it was not possible to achieve 100% contact between the sample and the halocarbon using this setup. Prior to the reaction, the sample was heated in 30 mL/min nitrogen flow to the reaction temperature. Then the gas flow was switched for CF_2Cl_2. After desired time, the gas flow was switched back to nitrogen, and the sample was purged with nitrogen for 2 min. Then, the ampule was taken out from the installation and filled with a solution of a spin probe.

1,3,5-Trinitrobenzene (TNB) and anthracene were used for characterization of electron-donor site and electron-acceptor sites, respectively. All the used reagents were of the "chemically pure" grade. Toluene was dried with activated alumina. The spin probes were adsorbed from 2×10^{-2} M solutions in toluene in air immediately after the samples were taken from the experimental installation and cooled down. Thereafter, the first EPR spectrum was recorded. Then, the samples were heated at 80 °C for 20 h before registering another EPR spectrum. All the EPR spectra were recorded at room temperature.

RESULTS AND DISCUSSION

Effect of Vanadium on the AP-MgO Reaction with CF_2Cl_2. Samples containing 1 and 10 wt % V in nanocrystalline MgO were prepared by mixing solid ammonium vanadate and AP-MgO-2. The textural parameters of the prepared samples are reported in Table 1. Calcination of the MgO aerogel sample without vanadium under vacuum at 500 °C following the procedure used for the synthesis of the vanadium-doped samples led to slight decrease of its surface area from 760 to 690 m^2/g (sample 5). Addition of 1% V followed by calcination at 550 °C did not lead to significant changes of the sample texture. Its calcination at 600 °C resulted in a minor decrease of the specific surface area. Meanwhile, the vanadium introduction in larger concentration (10 wt %) led to a significant decrease of the sample surface area to ~380 m^2/g. Meanwhile, the pore volume remained practically constant independent of the vanadium concentration.

Table 1. Textural Properties of Studied V_2O_5/AP-MgO-2 Samples

sample	vanadium concentration, %	calcination temperature, °C	surface area, m^2/g	pore volume, cm^3/g
1	10	550	376	0.54
2	10	450	382	0.50
3	1	550	684	0.55
4	1	600	630	0.58
5	0	500	760	0.59

The results of XRD study of these samples are reported in Table 2. The lattice parameters of all the studied AP-MgO samples were found to exceed the standard value for ideal MgO phase (4.2212, PC PDF ref. 45-0946). The lattice parameters of the samples containing vanadium were close to those of pure AP-MgO samples. So, the increase of the lattice parameter is probably due to the presence of residual anions in the oxygen framework after the aerogel synthesis procedure. The small particle size may also contribute to the change of the lattice parameter. As it was shown by XRD and high-resolution transmission electron microscopy (HRTEM) in our previous publications,[4,9,11] the MgO nanoparticles in our aerogels are mostly single-crystalline. So, their particle size is similar to the crystallite size determined by XRD.

Table 2. Phase Composition, Lattice Parameters, and Average Crystallite Sizes of the MgO Phase

sample	phase composition	lattice parameter, Å	crystallite size, Å
1	MgO, V_2O_5	4.228(2)	70
2	MgO, V_2O_5	4.228(2)	70
3	MgO	4.227(3)	65
4	MgO	4.230(3)	55
5	MgO	4.233(1)	60

The average particle size slightly increases after the vanadium introduction from 6 to 7 nm (Table 2). However, no changes that would evidence the existence of bulk interaction between the bulk MgO phase and the vanadium compounds were observed in the diffraction patterns.

No vanadium-containing phases were observed in the diffraction patterns of the samples with 1% V. The V_2O_5 phase was identified in addition to the MgO phase for the samples with 10% V. The average crystallite size of the V_2O_5 phase was about 20 nm and substantially exceeded that of the MgO phase. Meanwhile, no phases of mixed Mg−V oxides (magnesium vanadates) were observed by XRD. Still, we cannot exclude possible formation of small vanadate clusters not observable by XRD on the MgO surface. The phase composition of these samples is considerably different from those reported by us earlier for mixed magnesia-vanadia aerogels where uniform vanadium distribution in the MgO phase was observed until vanadium concentration exceeded 26 wt % (normalized for V_2O_5).[11,13]

dx.doi.org/10.1021/jp503916e | J. Phys. Chem. C 2014, 118, 13715−13725

The effect of vanadium concentration on the AP-MgO reaction with CF_2Cl_2 is shown in Figure 1. This reaction is

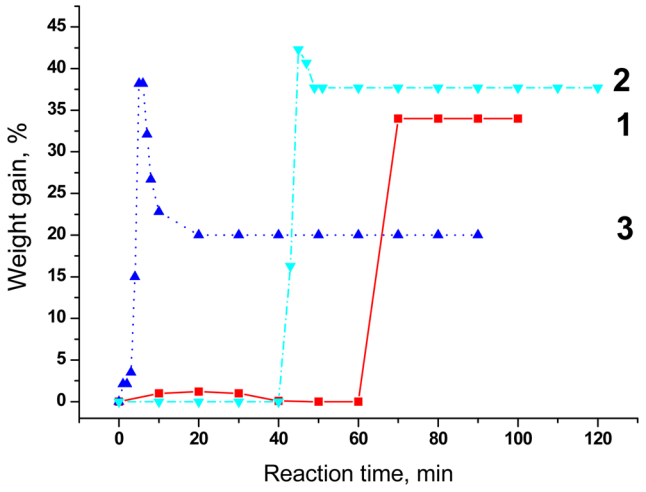

Figure 1. Effect of vanadium concentration on reaction between AP-MgO and CF_2Cl_2 at 400 °C: (1) AP-MgO-2, (2) 1%V/AP-MgO-2, (3) 10% V/AP-MgO-2.

characterized by a prolonged induction period preceding fast MgO conversion to MgF_2.[13,16] The XRD pattern of the sample after reaction is presented in Figure 2. MgF_2 appears to be the

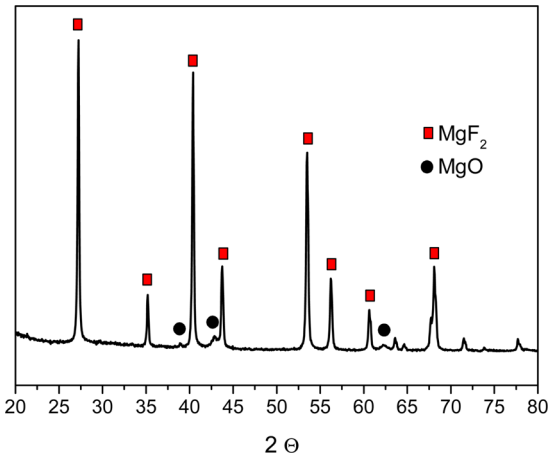

Figure 2. XRD pattern of the solid product obtained after the reaction of AP-MgO-2 with CF_2Cl_2.

only solid reaction product identifiable by XRD. Interestingly, some MgO nanoparticles never get involved in the reaction with the halocarbon and remain in the MgO phase.

Theoretical weight increase due to complete MgO conversion to MgF_2 is 55%. The weight gain of 34% observed in the experiment shown in Figure 1 corresponds to the MgO conversion degree of about 62%. Similar results were observed by us before. The exact fraction of the MgO nanoparticles in the reaction seems to depend on the type of the MgO sample, reaction conditions, choice of the reactor, and temperature. In different experiments, the weight gain varied from 10 to 40 wt % for AP-MgO nanoparticles. However, complete MgO conversion was never observed unless the reaction temperature was substantially increased.

It is not quite clear what prevents some of the MgO nanoparticles from getting involved into the solid-state reaction under conditions when a prolonged induction period is observed. The most plausible explanation is that the active state is formed due to the presence of certain active sites on the surface of most MgO nanoparticles. Apparently, such sites are not formed on the surface of the MgO nanoparticles that are not involved into the reaction.

Earlier we reported that CO_2 and CCl_4 were the main gaseous products formed in the AP-MgO reaction with CF_2Cl_2.[16] The analysis of the gas phase composition using an online gas chromatograph during the experiments reported in Figure 1 also showed the formation of CO_2 and CCl_4. However, the low time resolution of the chromatograph did not allow us to analyze details of the gas-phase composition changes during the active stage.

Such experiments were carried out by us earlier in different experimental installations.[13,16] Our experience suggests that the duration of the induction period can be very different in different installations, although in the same installation it is reproduced quite well. Very low but steady conversion of CF_2Cl_2 to CO_2 and CCl_4 formed in approximately equal molar amounts is observed during the induction period before the beginning of the active stage. Such reaction should be accompanied by the MgO conversion to MgF_2 according to reaction 1. This reaction is mostly limited to the surface, and its rate begins to increase toward the end of the induction period. Some chlorine atoms are retained on the MgO surface as well.[16]

$$2MgO + 2CF_2Cl_2 \rightarrow 2MgF_2 + CO_2 + CCl_4 \quad (1)$$

After the end of the induction period, the halocarbon conversion quickly increases in less than a minute. Sometimes the ratio of released CO_2 and CCl_4 is changed, so that the peaks of their release may not match.[13] The overall bulk reaction after the end of the induction period seems to be the sum of separate reactions 2 and 3. Magnesium chloride is formed as an intermediate, which usually does not form a separate phase. We observed it as an individual phase only when the reaction was carried out in a closed volume with an MgO excess.[16] In that case, reaction 3 was largely suppressed due to the CF_2Cl_2 deficit.

$$2MgO + CF_2Cl_2 \rightarrow MgCl_2 + MgF_2 + CO_2 \quad (2)$$

$$MgCl_2 + CF_2Cl_2 \rightarrow MgF_2 + CCl_4 \quad (3)$$

The introduction of only 1% V led to a substantial shortening of the induction period from 70 to 43 min (Figure 1). The MgO conversion increased to 69%. Such result is generally similar to the one reported by us earlier for AP-VOx-MgO aerogel samples synthesized by cogelation from alkoxides precursors.[13] Interestingly, the introduction of a small amount of vanadium by cogelation had greater impact on the length of the induction period compared to vanadium introduction in the form of ammonium vanadate used in this study.

Further increase of the vanadium concentration to 10 wt % led to even more significant shortening of the induction period down to 5 min (Figure 1). The vanadium doping also led to the appearance of a typical hump on the kinetic curve. The maximum weight obtained after the active phase of the reaction somewhat decreased in the following several minutes. In our installation we observed this feature only if vanadium was present in the samples. In a different setup with higher sensitivity, it was also observed for pure MgO.[13] In that case, it was argued that this hump is related to substitution of chlorine atoms introduced into MgO due to reaction 2 during the active

dx.doi.org/10.1021/jp503916e | J. Phys. Chem. C 2014, 118, 13715−13725

phase for fluorine atoms according to reaction 3. Fluorine is lighter than chlorine, so this reactions results in some weight loss. Substitution may either take place during the active phase of the bulk reaction or following it. In the latter case, a hump on the kinetic curve is observed.

For samples with high vanadium concentrations, additional weight loss may result from the release of volatile vanadium compounds, e.g., $VOCl_3$. This may be the reason for lower weight gain after reaction of the 10 wt % V/MgO sample with CF_2Cl_2 (Figure 1). This effect was larger in this study, where V_2O_5 was observed as a separate phase from that for the samples prepared earlier by the cogelation method.[13] In the latter case, vanadium was uniformly distributed in the material without forming an individual phase.

Substitution of the inert gas flow used for the sample activation for oxygen had practically no effect on the kinetics of the reaction with CF_2Cl_2 (Figure 3). When the sample was

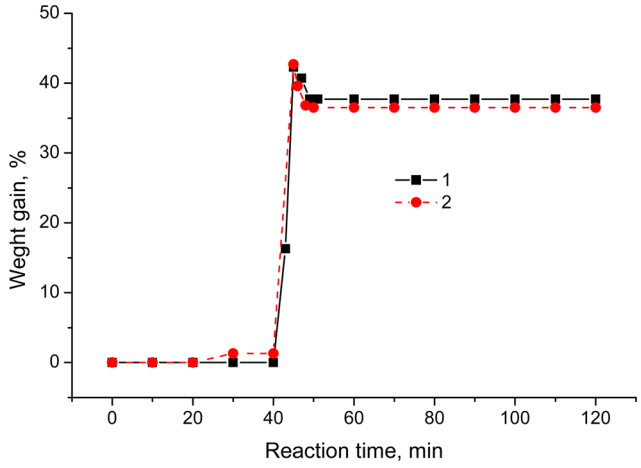

Figure 3. Effect of the gas used for activation of 1%V/AP-MgO-2 on the kinetics of its reaction with CF_2Cl_2 at 400 °C: (1) Ar, (2) O_2.

activated in a reducing atmosphere (hydrogen flow), only minor and poorly reproducible changes of the induction period length were observed. As the vanadium oxidation state in dispersed oxide materials is known to depend significantly on the pretreatment conditions, these results indicate that its oxidation state does not substantially affect the kinetics of the reaction with the halocarbon. So, this is most likely not a redox reaction even in the presence of the transition metal.

The obtained data on the reaction kinetics reveal the following interesting phenomenon. In this study, vanadium was not homogeneously distributed in the MgO phase. Some of it was present in the form of V_2O_5, and some was apparently dispersed as vanadate clusters on the surface of the MgO nanoparticles. As MgO nanoparticles are very small (1−5 nm), many of them were probably not doped with vanadium at all, particularly at low vanadium concentration. In this case, one could imagine that the kinetics of reaction between VOx-MgO and CF_2Cl_2 would consist of two or more steps. If the length of the induction period simply depended on the vanadium concentration on the surface, the induction period would be shortened only for vanadium-doped nanoparticles. Meanwhile, it would remain almost the same for the nanoparticle containing no or relatively little vanadium. In fact, a whole distribution of the induction periods could be obtained. However, the experiments showed a completely different result: the induction period was always shifted in one piece. Whenever the active phase of the reaction started, all the MgO nanoparticles inclined to react were converted in a relatively short period of time.

Effect of Carbon Coating on the AP-MgO Reaction with Halocarbons. Earlier it was demonstrated that the coverage of MgO aerogels with a porous carbon coating improved their stability in the presence of water and increased usable time of storage in air under ambient conditions compared to AP-MgO without such coating.[1] It was shown that carbon deposition on nanocrystalline MgO aerogels by decomposition of hydrocarbons is an easily controllable procedure, yielding surface carbon coating with high surface area.[40] The surface active sites of such materials were studied by EPR. C/AP-MgO samples with the carbon coating above 10 wt % were found to preserve surface active sites capable of initiating destructive sorption of halogenated compounds.[26] So, it was interesting to study how such carbon coating affects the AP-MgO reaction with halocarbons. Our initial assumption was that the carbon coating would hamper this reaction or completely prevent it from taking place.

However, a completely different result was obtained. It was found that carbon-coated AP-MgO samples actually reacted faster with halocarbons than the samples without carbon. The duration of the induction period during reaction of the studied AP-MgO sample with CF_2Cl_2 at 400 °C was little bit shorter than 1 h (Figure 4). The introduction of just 1 wt % C led to

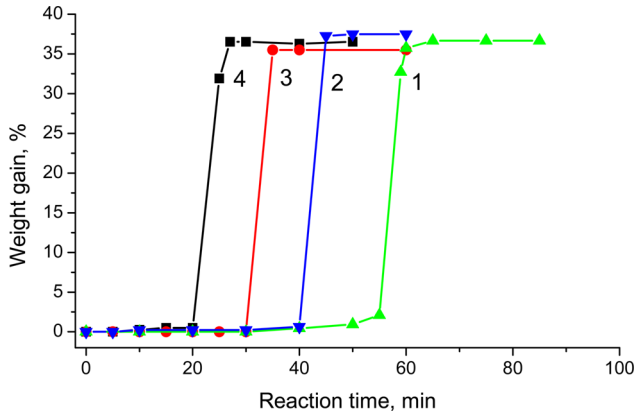

Figure 4. Effect of modification with carbon on the kinetics of AP-MgO-1 reaction with CF_2Cl_2 at 400 °C: 0 (1), 1 (2), 3 (3), and 10% C (4).

unexpected shortening of the induction period to 40 min while the MgO conversion was preserved (Figure 4). Further increase of the carbon concentration to 10 wt % made the induction even shorter. Its minimum duration observed in our experiments over carbon-coated AP-MgO was about 20 min, i.e., approximately 3 times shorter than that over AP-MgO without the carbon modification.

These results mean that, despite partial screening of the MgO surface with porous carbon, the whole volume of the sorbent remains accessible for the reaction with the halocarbon. Apparently, accumulation of the active sites accounting for the end of the induction period and beginning of the active reaction phase occurs faster in the presence of the carbon coating.

Similar results were obtained with another halocarbon, $CFCl_3$ (Figure 5). The induction period was not expressed so clearly in this system. Apparently, this is related to a different

dx.doi.org/10.1021/jp503916e | J. Phys. Chem. C 2014, 118, 13715−13725

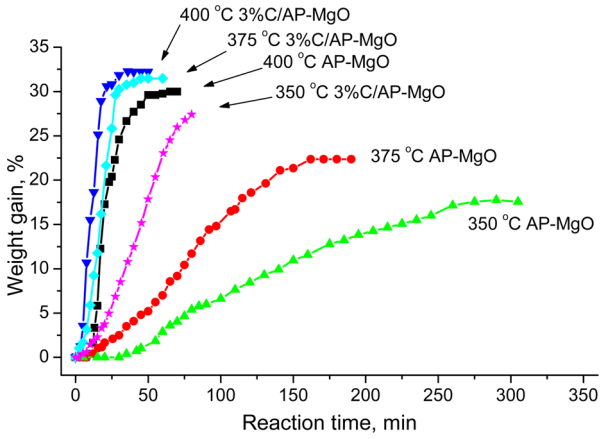

Figure 5. Effect of temperature on the kinetics of reaction between AP-MgO-1 and 3%C/AP-MgO-1 with $CFCl_3$.

Cl/F ratio in the halocarbon molecule, which led to less overheating of the sample during the active phase of the reaction. As it was shown by us earlier, the sample overheating after the end of the induction period is responsible for the unusually fast active phase in the reaction between AP-MgO and CF_2Cl_2.[13,20]

It is notable that at all temperatures between 350 and 400 °C the introduction of 3 wt % C both shortened the induction period and increased the AP-MgO conversion (Figure 5). The largest weight gain (32 wt %) was observed after reaction at 400 °C for the sample modified with carbon. However, this value corresponds to only 60% MgO conversion, which is somewhat lower than in the case of the reaction with CF_2Cl_2 (Figure 4).

As we have shown above, vanadium addition can shorten the induction during the MgO reaction with CF_2Cl_2 both when vanadium is finely dispersed in the MgO phase[13] and when it is present as a separate phase. We also studied how the method of carbon addition to AP-MgO affected its reactivity to CF_2Cl_2. We prepared a mechanical mixture of AP-MgO with 5 wt % of activated carbon with specific surface 860 m^2/g and commercial graphite with the surface area 10 m^2/g. The performance of these mixtures was compared with that of carbon-coated AP-MgO with the same carbon concentration and pure AP-MgO.

The addition of activated carbon to AP-MgO proved to be as effective with respect to its reaction with CF_2Cl_2 as preparation of a porous carbon coating on the AP-MgO surface (Figure 6).

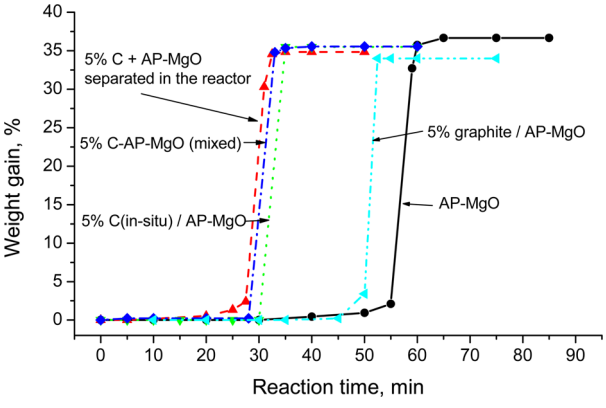

Figure 6. Effect of the method used for carbon addition to AP-MgO-1 on the kinetics of reaction between 5%C/AP-MgO and CF_2Cl_2 at 400 °C.

The induction period observed for the mechanical mixture containing 5 wt % of activated carbon was shorter by 2 min than that obtained for the sample with the same amount of carbon prepared as a carbon coating of the surface of AP-MgO by butadiene decomposition (33 and 35 min, respectively). It was shorter by more than 20 min than in the case of MgO aerogel without carbon. The MgO conversion also did not seem to depend on the carbon introduction method. Interestingly, the addition of graphite with low surface also led to shortening of the induction, although its effect was weaker (Figure 6).

Similar reactivity of the C/AP-MgO samples prepared by decomposition of hydrocarbons in situ and by mixing with activated carbon seems to indicate that the halocarbons react with carbon and MgO independently. It is hard to imagine that some active species could move directly from the carbon surface to MgO without passing through the gas phase, particularly in the case of the sorbents prepared by mechanical mixing.

To confirm this hypothesis, we studied the reaction of CF_2Cl_2 with AP-MgO samples containing 5 wt % of activated carbon where the MgO and C phases were not mixed at all. Instead, carbon was either placed directly above or below the MgO sample or was even located completely separately in the sample holder. In the latter case, the MgO and carbon phases did not have any physical contact at all.

It was found that the duration of the induction period and the MgO conversion did not depend on the relative location of the activated carbon and AP-MgO samples. The same results within the experimental error were obtained for the samples where these phases were carefully mixed, placed on top of each other, and located separately. The kinetic curve obtained for the samples with the separate location of the phases is shown in Figure 6 for comparison.

Characterization of Electron-Donor and Electron-Acceptor Sites during AP-MgO Reaction with CF_2Cl_2. High activity of nanocrystalline MgO aerogels is traditionally attributed to high concentration of low-coordinated ions on their surface.[3] However, the obtained data for the reaction with CF_2Cl_2 vividly demonstrate that the active form of the destructive sorbent is formed only after the induction period. Apparently, during the induction period, certain active sites not existing before reaction are accumulated on the MgO surface. Bulk transformation of magnesium oxide to magnesium fluoride begins only when such sites are formed in sufficient concentration. Their activity must be relatively high to counteract considerable loss of the sorbent specific surface area earlier observed during the induction period.[16]

A similar situation was observed by us during catalytic dehydrohalogenation of 1-chlorobutane and 1-iodobutane over nanocrystalline MgO.[1,10,15,17] Very active sites with acidic properties were formed during the initial stages of these reactions. These sites proved to be 1−2 orders of magnitude more active in catalytic dehydrohalogenation than the sites present on the surface of AP-MgO. During these reactions, the surface and bulk of the MgO nanoparticles are modified with the halogen ions. As a similar effect is observed during the induction period of the AP-MgO reaction with CF_2Cl_2,[16] it is very likely that the active sites of both processes may be similar.

The data presented above suggest that some unknown intermediates forming on the surface of activated carbon and vanadia can be transferred through the gas phase to react with AP-MgO. This reaction results in faster formation of the surface

dx.doi.org/10.1021/jp503916e | J. Phys. Chem. C 2014, 118, 13715−13725

active sites, which initiate the fast bulk reaction between AP-MgO and CF_2Cl_2. In the absence of carbon or vanadia, such sites are also gradually accumulated, although this process is substantially slower.

Vanadia is a transition metal oxide known for its activity in selective catalytic oxidation.[9,18,19,42−46] Surface vanadyl groups with oxidative properties are commonly believed to account for the catalytic activity of supported vanadia catalysts. However, there are many results suggesting that bridging oxygen atoms might be the active species.[47] In addition, O^- radicals are readily observed by EPR during reoxidation of reduced VO_x/SiO_2 catalysts.[48−50] We have recently shown by DFT calculations that oxygen isotopic exchange on supported vanadia might be initiated on the surface O^- radicals.[51,52] These results suggest that oxygen radicals may be present on the surface of oxidation catalysts under catalytic conditions and account for the activity in catalytic and destructive sorption reactions.

Meanwhile, carbon does not possess oxidative properties. So, the origin of the positive effect of carbon on the reactivity of nanocrystalline MgO is not quite clear. Most likely, its surface contains active sites initiating abstraction of a chlorine atom or ion from the halocarbon molecule. These could be acidic surface groups known to exist on the surface of activated carbon, which might be able to hydrolyze CF_2Cl_2. The products of this slow reaction are transferred through the gas phase to the MgO surface, where they react easier than CF_2Cl_2, which is very chemically inert. This reaction leads to gradual accumulation of active sites on its surface, which react with CF_2Cl_2 very fast. When their concentration becomes sufficiently high, the fast bulk destructive sorption of the halocarbon begins. Then, this reaction is self-accelerated because it is exothermal.

Various potentially active surface sites have been identified on the MgO surface. In addition to fairly conventional basic sites and low-coordinated surface ions, these are highly active oxygen radical anions, electron-donor sites capable of donating an electron to TNB and acid sites identified using stable nitroxyl radicals.[26,28,29,53,54] Additional studies of changes in the concentrations of different active sites were required to determine the nature of the active sites accounting for the fast reaction between MgO and halocarbons.

The unexpected activity of carbon and the fact that vanadium addition only shortened the induction period rather than eliminated it altogether suggest that oxygen radicals are unlikely candidates for the role of the active sites in this reaction. So, our special interest was attracted to electron-donor and electron-acceptor sites, which definitely have high chemical activity. Earlier we found direct correlations between the concentrations of such sites on the surface of catalysts and their catalytic activity in low-temperature CO oxidation, *n*-butane isomerization and ethanol dehydration.[30,36,37,55]

The EPR spectra observed after TNB adsorption on AP-MgO samples subjected to reaction with CF_2Cl_2 for different periods of time are shown in Figure 7. A strong signal of TNB radical anions was observed on the AP-MgO sample after activation in nitrogen flow without any reaction. The signal was characterized by anisotropic splitting with A_{zz} = 27.2 G on one nitrogen atom. The splitting is slighter smaller than that earlier reported after adsorption of 1,3-dinitrobenzene (DNB) on the same material (28.5 G).[26] The smaller splitting results from the presence of three nitro groups in TNB instead of just two in DNB. A similar decrease of the spitting was recently reported

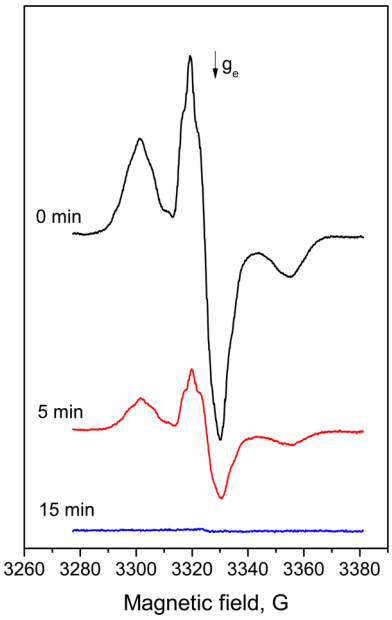

Figure 7. EPR spectra observed after TNB adsorption from toluene solution on AP-MgO-2 subjected to reaction with CF_2Cl_2 for different times.

by us for the radical anions of TNB and DNB observed on the surface of γ-Al_2O_3 (31.1 and 33.2 G, respectively).[25] The larger splitting on the alumina surface, which was confirmed by quantum chemical simulations, is apparently due to higher electronegativity of aluminum.

The intensity of the EPR signal observed after TNB adsorption on activated AP-MgO-2 was about 6×10^{18} g^{-1}. This value corresponds to the concentration of electron-donor sites present on the surface after the used activation procedure, which were capable of direct electron transfer to TNB molecules. The ionization process on the MgO was different from the one observed on alumina. The signal of the radical anions appeared immediately after the TNB adsorption, and its intensity quickly decreased thereafter. Meanwhile, no signal was observed on alumina after TNB adsorption. It slowly appeared after some time. To reach the maximum concentration of TNB radical anions on the γ-Al_2O_3 surface, one has to heat the sample at 80 °C for several hours, wait at room temperature for several days, or subject it to illumination with visible light.[25,29] So, the strength of the electron-donor sites on the MgO surface appears to be higher than on γ-Al_2O_3. This result is in good agreement with the assumption that the strength of these sites correlates with the sample basicity.

The concentration of electron-donor sites tested using TNB as the spin probe gradually decreased during reaction between AP-MgO and CF_2Cl_2 (Figure 7). It took 10−15 min for the signal to disappear on all studied samples, independent of the length of the induction period observed on them. Their concentration decreased during the induction period, and no correlation between the induction period duration and the concentration of the electron-donor sites was observed. So, despite the obvious activity of the electron-donor sites in the electron-transfer reaction, they are hardly involved in the bulk reaction between nanocrystalline MgO and CF_2Cl_2.

On the contrary, the concentration of weak electron-acceptor sites tested using anthracene as the spin probe qualitatively follows changes in the activity in the solid-state reaction.

dx.doi.org/10.1021/jp503916e | J. Phys. Chem. C 2014, 118, 13715−13725

Anthracene sorption on AP-MgO-2 after activation in nitrogen does not reveal the presence of any electron-acceptor sites. The observed weak EPR signal (Figure 8) belongs to intrinsic

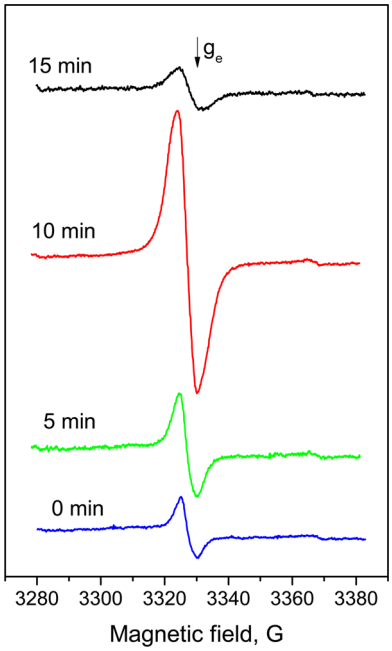

Figure 8. EPR observed on AP-MgO-2 subjected to reaction with CF_2Cl_2 for different times after anthracene adsorption from toluene solution followed by heating at 80 °C for 20 h.

defects present in AP-MgO, which were discussed in detail earlier.[28] It is not altered even by heating at 80 °C that was reported to reveal weak acceptor sites accounting for ethanol dehydration.[37] Meanwhile, such heat treatment leads to the appearance of a singlet at $g = 2.003$ on the samples subjected to reaction with CF_2Cl_2 for different periods of time (Figure 8). This signal can be attributed to coke precursors formed by polycondensation of aromatic donor molecules on weak electron-acceptor sites.[21,37]

The intensities of the EPR signal at $g \sim 2.003$ observed immediately after anthracene adsorption on AP-MgO-2 samples subjected to reaction with CF_2Cl_2 for different periods of time and after additional heating at 80 °C for 20 h are presented in Figure 9. The signal registered on most samples after anthracene adsorption is similar to the one observed on AP-MgO-2 before reaction with the halocarbon. Its intensity slightly decreases during the induction period. However, it is clearly observed on all samples taken from the reactor before the end of the induction period. So, the line in Figure 9 corresponding to intensities obtained by double integration of this signal can be treated as a baseline before generation of radical cations on electron-acceptor sites.

No additional EPR signals resulting from the interaction with the spin probe were observed until the reaction time of 10 min. This sample was characterized by the appearance of a symmetrical EPR signal with approximately the same g-factor and higher intensity resulting from anthracene ionization followed by polycondensation via the radical cation mechanism. Its intensity exceeded that of the intrinsic EPR signal approximately by a factor of 3. At longer reaction times, this signal practically disappeared. This means that electron-acceptor sites with intermediate strength capable of ionizing

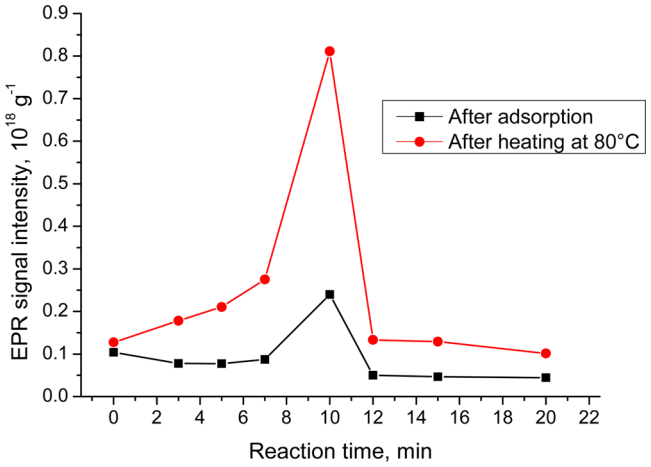

Figure 9. Dependence of the intensities of EPR spectra observed after anthracene adsorption from toluene solution on AP-MgO-2 on time of their reaction with CF_2Cl_2.

anthracene immediately after adsorption were present only on the AP-MgO sample subjected to reaction with CF_2Cl_2 for 10 min. Clearly, the properties of this sample were different from the samples subjected to reaction both for shorter and longer periods of time.

After heating the samples with adsorbed anthracene at 80 °C, the singlet EPR signal attributable to paramagnetic polyaromatic species formed on weak electron-acceptor sites appeared on all the AP-MgO samples that contacted with CF_2Cl_2. Such heating initiates slow formation of larger aromatic species having lower ionization potentials than anthracene. They can be ionized on weaker electron-acceptor sites when their ionization potential becomes sufficiently low. The original signal belonging to intrinsic paramagnetic defects remained the same only on the sample that did not react with CF_2Cl_2. The minor difference in the intensities of EPR signal on this sample before and after calcination is within the experimental error. Apparently, the surface of nanocrystalline MgO lacks even such weak electron-acceptor sites.

Meanwhile, comparison of the two data sets presented in Figure 9 proves the formation of additional paramagnetic species on the samples subjected to reaction with CF_2Cl_2 even for short periods of time. If the maximum intensity observed after 10 min reaction corresponds to the active state after the end of the induction period, the concentration of such weak electron-acceptor sites increases even during the induction period when few other changes with the sample take place. Assuming that no such sites exist on the sample before reaction and subtracting the intensity of the EPR spectrum observed on this sample, one can see that the concentration of weak electron-acceptor sites on the surface of the sample subjected to reaction with CF_2Cl_2 for 7 min is ca. 3 times higher than in the case of the 3 min reaction. Then, this intensity jumps up by another factor of 3 for the 10 min sample before going down for the samples subjected to reaction with CF_2Cl_2 for longer periods of time.

The obtained data show that the sample subjected to reaction with CF_2Cl_2 for 10 min is quite unique with the highest concentration of weak electron-acceptor sites and the presence of sites with intermediate strength. Although we were not able to simultaneously monitor the weight of the sample and determine the length of the induction period independently, we are quite confident that it was about 10 min in this

dx.doi.org/10.1021/jp503916e | J. Phys. Chem. C 2014, 118, 13715−13725

installation. Visible changes occurring with the sample volume, which most likely correspond to bulk chemical reaction, took place at the same moment. This experimental setup was optimized to obtain the shortest and reproducible length of the induction period. So, we are not surprised that it was much shorter in this installation than in the McBain balance. Our previous experience suggests that the length of the induction period substantially depends on the used experimental installation.

These results clearly demonstrate that weak electron-acceptor sites are accumulated on the MgO surface during the induction period of its reaction with CF_2Cl_2. Apparently such sites are somehow related to fluorine and/or chlorine atoms that were reported to be accumulated on the MgO surface during the induction period.[16] Alumina modification with chorine also increased the concentration of similar weak electron-acceptor sites tested using anthracene adsorption followed with heating at 80 °C.[37] These electron-acceptor sites are the first genuinely active sites, whose concentration grows during the induction period and reaches a maximum during the active phase. Furthermore, some stronger electron-acceptor sites are present only in the active state, as is evidenced by immediate anthracene ionization on the sample subjected to reaction with CF_2Cl_2 for 10 min. So, at the moment they seem to be the most likely candidates for the role of surface active sites initiating the solid-state reaction between nanocrystalline MgO and CF_2Cl_2.

The problem is that these sites are identified only by their reactivity in the single electron transfer. Electron-acceptor sites capable of generating radical cations after adsorption of aromatic molecules have been known since 1960s, mostly for acidic oxides and zeolites.[21,24] Their structure is not known for certain, even for materials where they have been extensively studied. Several hypotheses on their nature have been suggested. According to the most common suggested theories, the electron-acceptor sites could be Lewis acid sites accepting a single electron rather than an electron pair,[56] Bronsted acid sites,[37] or O^- radicals.[21,57] Such sites were never previously reported for MgO or chlorinated/fluorinated MgO. More experimental and theoretical studies are required for understanding the properties of electron-acceptor sites on the surface of halogenated MgO and the mechanism or their possible involvement in the reaction with CF_2Cl_2.

CONCLUSIONS

We found that vanadia added to nanocrystalline MgO in the form of surface clusters or even a separate phase shortens the induction period in the reaction with CF_2Cl_2, quite similarly to vanadia homogeneously mixed with MgO. Even more intriguing results were obtained over carbon-doped nanocrystalline MgO. Although carbon itself was not involved into a bulk reaction with CF_2Cl_2, it somehow shortened the induction period. This effect did not depend on the location of the active carbon layer relative to MgO.

We believe that some intermediates are generated from the halocarbon on the surface of vanadia and carbon. Then, these intermediates are transported through the gas phase to MgO, where they react easier than the original CF_2Cl_2. Most likely, these are some oxygenated compounds, such as CF_2O, CF_2ClOH, etc.

The reported results clearly demonstrate that surface active sites formed during the induction period of reaction between nanocrystalline pure or modified MgO samples and halocarbons account for beginning of the fast bulk reaction. Note that even the concept that active sites with specific chemical properties are responsible for solid-state chemical reactions is rarely used in solid-state chemistry. Usually such reactions are attributed to the presence of certain defects of the crystalline structure.

In catalysis, considerable knowledge has been accumulated on the properties and structure of various active sites existing on the surface. Today it is generally accepted that catalytic reactions are initiated on specific surface active sites. Often the properties of such sites are well-known. We believe that the same approach should be extended to solid-state reactions. Thorough investigation of correlations between rates of such reactions and concentrations of various active sites using methods and approaches developed for characterization of the catalyst surface should ultimately reveal the nature of surface sites where various bulk reactions are initiated. The results reported in this paper seem to be a first major step toward this goal.

The obtained results do not yet prove that weak electron-acceptor sites are responsible for the beginning of the bulk reaction between nanocrystalline MgO and CF_2Cl_2. However, currently they are the most likely candidates for the role of surface sites responsible for such abrupt change of the reaction mechanism. Obviously, a more comprehensive study of the role of electron-acceptor sites in this process involving more samples, including doped ones, and more spin probes is required to give a definitive answer. Such study is currently under way in our laboratories, and its results will be reported elsewhere.

AUTHOR INFORMATION

Corresponding Author

*E-mail: abedilo@bk.ru; Telephone: +7-383-326-9421; Fax: +7-383-330-8056.

Notes

The authors declare no competing financial interest.

ACKNOWLEDGMENTS

The authors are grateful to M.S. Mel'gunov and S.V. Tsybulya for participation in the experiments and useful discussions. This study was supported in part by Russian Foundation for Basic Research (Grants 12-03-00905-a and 13-03-12227-ofi-m).

REFERENCES

(1) Bedilo, A. F.; Sigel, M. J.; Koper, O. B.; Melgunov, M. S.; Klabunde, K. J. Synthesis of Carbon-Coated MgO Nanoparticles. *J. Mater. Chem.* **2002**, *12*, 3599−3604.

(2) Jiang, Y.; Decker, S.; Mohs, C.; Klabunde, K. J. Catalytic Solid State Reactions on the Surface of Nanoscale Metal Oxide Particles. *J. Catal.* **1998**, *180*, 24−35.

(3) Klabunde, K. J.; Stark, J.; Koper, O.; Mohs, C.; Park, D. G.; Decker, S.; Jiang, Y.; Lagadic, I.; Zhang, D. J. Nanocrystals as Stoichiometric Reagents with Unique Surface Chemistry. *J. Phys. Chem.* **1996**, *100*, 12142−12153.

(4) Richards, R.; Li, W. F.; Decker, S.; Davidson, C.; Koper, O.; Zaikovski, V.; Volodin, A.; Rieker, T.; Klabunde, K. J. Consolidation of Metal Oxide Nanocrystals. Reactive Pellets with Controllable Pore Structure that Represent a New Family of Porous, Inorganic Materials. *J. Am. Chem. Soc.* **2000**, *122*, 4921−4925.

(5) Stoimenov, P. K.; Klinger, R. L.; Marchin, G. L.; Klabunde, K. J. Metal Oxide Nanoparticles as Bactericidal Agents. *Langmuir* **2002**, *18*, 6679−6686.

(6) Decker, S.; Klabunde, K. J. Enhancing Effect of Fe_2O_3 on the Ability of Nanocrystalline Calcium Oxide to Adsorb SO_2. *J. Am. Chem. Soc.* **1996**, *118*, 12465−12466.
(7) Bedilo, A. F.; Klabunde, K. J. Synthesis of High Surface Area Zirconia Aerogels Using High Temperature Supercritical Drying. *Nanostruct. Mater.* **1997**, *8*, 119−135.
(8) Bedilo, A. F.; Klabunde, K. J. Synthesis of Catalytically Active Sulfated Zirconia Aerogels. *J. Catal.* **1998**, *176*, 448−458.
(9) Chesnokov, V. V.; Bedilo, A. F.; Heroux, D. S.; Mishakov, I. V.; Klabunde, K. J. Oxidative Dehydrogenation of Butane over Nanocrystalline MgO, Al_2O_3, and VOx/MgO Catalysts in the Presence of Small Amounts of Iodine. *J. Catal.* **2003**, *218*, 438−446.
(10) Gupta, P. P.; Hohn, K. L.; Erickson, L. E.; Klabunde, K. J.; Bedilo, A. F. Transformation of Nanocrystalline MgO Pellets in Reaction with 1-Chlorobutane. *AlChE J.* **2004**, *50*, 3195−3205.
(11) Ilyina, E. V.; Mishakov, I. V.; Vedyagin, A. A.; Cherepanova, S. V.; Nadeev, A. N.; Bedilo, A. F.; Klabunde, K. J. Synthesis and Characterization of Mesoporous VOx/MgO Aerogels with High Surface Area. *Microporous Mesoporous Mater.* **2012**, *160*, 32−40.
(12) Ilyina, E. V.; Mishakov, I. V.; Vedyagin, A. A.; Bedilo, A. F. Aerogel Method for Preparation of Nanocrystalline CoOx MgO and VOx MgO Catalysts. *J. Sol−Gel Sci. Technol.* **2013**, *68*, 423−428.
(13) Ilyina, E. V.; Mishakov, I. V.; Vedyagin, A. A.; Bedilo, A. F.; Klabunde, K. J. Promoting Effect of Vanadium on CF_2Cl_2 Destructive Sorption over Nanocrystalline Mesoporous MgO. *Microporous Mesoporous Mater.* **2013**, *175*, 76−84.
(14) Koper, O. B.; Wovchko, E. A.; Glass, J. A.; Yates, J. T.; Klabunde, K. J. Decomposition of CCl_4 on CaO. *Langmuir* **1995**, *11*, 2054−2059.
(15) Mishakov, I. V.; Bedilo, A. F.; Richards, R. M.; Chesnokov, V. V.; Volodin, A. M.; Zaikovskii, V. I.; Buyanov, R. A.; Klabunde, K. J. Nanocrystalline MgO as a Dehydrohalogenation Catalyst. *J. Catal.* **2002**, *206*, 40−48.
(16) Mishakov, I. V.; Zaikovskii, V. I.; Heroux, D. S.; Bedilo, A. F.; Chesnokov, V. V.; Volodin, A. M.; Martyanov, I. N.; Filimonova, S. V.; Parmon, V. N.; Klabunde, K. J. CF_2Cl_2 Decomposition over Nanocrystalline MgO: Evidence for Long Induction Periods. *J. Phys. Chem. B* **2005**, *109*, 6982−6989.
(17) Mishakov, I. V.; Heroux, D. S.; Chesnokov, V. V.; Koscheev, S. G.; Mel'gunov, M. S.; Bedilo, A. F.; Buyanov, R. A.; Klabunde, K. J. Reaction of Nanocrystalline MgO with 1-Iodobutane. *J. Catal.* **2005**, *229*, 344−351.
(18) Mishakov, I. V.; Ilyina, E. V.; Bedilo, A. F.; Vedyagin, A. A. Nanocrystalline Aerogel VOx/MgO as a Catalyst for Oxidative Dehydrogenation of Propane. *React. Kinet. Catal. Lett.* **2009**, *97*, 355−361.
(19) Mishakov, I. V.; Vedyagin, A. A.; Bedilo, A. F.; Zailovskii, V. I.; Klabunde, K. J. Aerogel VOx/MgO Catalysts for Oxidative Dehydrogenation of Propane. *Catal. Today* **2009**, *144*, 278−284.
(20) Mishakov, I. V.; Vedyagin, A. A.; Bedilo, A. F.; Mel'gunov, M. S.; Buyanov, R. A. A Study of the Reaction of CF_2Cl_2 with Nanocrystalline MgO on a TEOM Microanalyzer. *Dokl. Phys. Chem.* **2006**, *410*, 251−254.
(21) Bedilo, A. F.; Volodin, A. M. Radical Cations of Aromatic Molecules with High Ionization Potentials on the Surfaces of Oxide Catalysts: Formation, Properties, and Reactivity. *Kinet. Catal.* **2009**, *50*, 314−324.
(22) Flockhart, B. D.; Leith, I. R.; Pink, R. C. Evidence for the Redox Nature of the Surface of Catalytic Aluminas. *J. Catal.* **1967**, *9*, 45−50.
(23) Flockhart, B. D.; Leith, I. R.; Pink, R. C. Electron-Transfer at Alumina Surfaces. Part 3. Reduction of Aromatic Nitro-Compounds. *Trans. Faraday Soc.* **1970**, *66*, 469−476.
(24) Garcia, H.; Roth, H. D. Generation and Reactions of Organic Radical Cations in Zeolites. *Chem. Rev.* **2002**, *102*, 3947−4007.
(25) Medvedev, D. A.; Rybinskaya, A. A.; Kenzhin, R. M.; Volodin, A. M.; Bedilo, A. F. Characterization of Electron Donor Sites on Al_2O_3 Surface. *Phys. Chem. Chem. Phys.* **2012**, *14*, 2587−2598.
(26) Heroux, D. S.; Volodin, A. M.; Zaikovski, V. I.; Chesnokov, V. V.; Bedilo, A. F.; Klabunde, K. J. ESR and HRTEM Study of Carbon-Coated Nanocrystalline MgO. *J. Phys. Chem. B* **2004**, *108*, 3140−3144.
(27) Konovalova, T. A.; Bedilo, A. F.; Volodin, A. M. ESR Studies of Nitroxyl Radicals Tempon and M-Dinitrobenzene Molecules Adsorbed on Gamma-Al_2O_3. *React. Kinet. Catal. Lett.* **1993**, *51*, 81−86.
(28) Richards, R. M.; Volodin, A. M.; Bedilo, A. F.; Klabunde, K. J. ESR Study of Nanocrystalline Aerogel-Prepared Magnesium Oxide. *Phys. Chem. Chem. Phys.* **2003**, *5*, 4299−4305.
(29) Volodin, A. M. Photoinduced Phenomena on the Surface of Wide-Band-Gap Oxide Catalysts. *Catal. Today* **2000**, *58*, 103−114.
(30) Vedyagin, A. A.; Volodin, A. M.; Stoyanovskii, V. O.; Mishakov, I. V.; Medvedev, D. A.; Noskov, A. S. Characterization of Active Sites of Pd/Al_2O_3 Model Catalysts with Low Pd Content by Luminescence, EPR and Ethane Hydrogenolysis. *Appl. Catal. B: Environ.* **2011**, *103*, 397−403.
(31) Bedilo, A. F.; Volodin, A. M.; Zenkovets, G. A.; Timoshok, G. V. Formation of Cation Radicals from Methylbenzenes on Sulfated Zirconia. *React. Kinet. Catal. Lett.* **1995**, *55*, 183−190.
(32) Bedilo, A. F.; Kim, V. I.; Volodin, A. M. Effect of Light on Reactions over Sulfated Zirconia. *J. Catal.* **1998**, *176*, 294−304.
(33) Bedilo, A. F.; Volodin, A. M. Suppression of Radical-Cationic Benzene Oligomerization on Sulfated Zirconia. *React. Kinet. Catal. Lett.* **1999**, *67*, 197−203.
(34) Bedilo, A. F.; Timoshok, A. V.; Volodin, A. M. Formation of Tetramethylethylene Radical Cations after Pentane Adsorption on Sulfated Zirconia. *Catal. Lett.* **2000**, *68*, 209−214.
(35) Timoshok, A. V.; Bedilo, A. F.; Volodin, A. M. Cation Radical Intermediates in Benzene and Toluene Polycondensation on Sulfated Zirconia. *React. Kinet. Catal. Lett.* **1996**, *59*, 165−171.
(36) Bedilo, A. F.; Ivanova, A. S.; Pakhomov, N. A.; Volodin, A. M. Development of an ESR Technique for Testing Sulfated Zirconia Catalysts. *J. Mol. Catal. A: Chem.* **2000**, *158*, 409−412.
(37) Zotov, R. A.; Molchanov, V. V.; Volodin, A. M.; Bedilo, A. F. Characterization of the Active Sites on the Surface of Al_2O_3 Ethanol Dehydration Catalysts by EPR Using Spin Probes. *J. Catal.* **2011**, *278*, 71−77.
(38) Martyanov, I. N.; Klabunde, K. J. Decomposition of CCl_3F over Vanadium Oxides and $[MgV_xO_y]MgO$ Shell/Core-Like Particles. *J. Catal.* **2004**, *224*, 340−346.
(39) Tamai, T.; Inazu, K.; Aika, K. Enhanced Dichlorodifluoromethane Decomposition with Selective Fluorine Absorption by Acidic Fluorinated Magnesium Oxide. *Bull. Chem. Soc. Jpn.* **2004**, *77*, 1239−1247.
(40) Mel'gunov, M. S.; Mel'gunova, E. A.; Zaikovskii, V. I.; Fenelonov, V. B.; Bedilo, A. F.; Klabunde, K. J. Carbon Dispersion and Morphology in Carbon-Coated Nanocrystalline MgO. *Langmuir* **2003**, *19*, 10426−10433.
(41) Bolshov, V. A.; Volodin, A. M.; Zhidomirov, G. M.; Shubin, A. A.; Bedilo, A. F. Radical Intermediates in the Photoinduced Formation of Benzene Cation-Radicals over H-ZSM-5 Zeolites. *J. Phys. Chem.* **1994**, *98*, 7551−7554.
(42) Beck, B.; Harth, M.; Hamilton, N. G.; Carrero, C.; Uhlrich, J. J.; Trunschke, A.; Shaikhutdinov, S.; Schubert, H.; Freund, H. J.; Schlogl, R.; et al. Partial Oxidation of Ethanol on Vanadia Catalysts on Supporting Oxides with Different Redox Properties Compared to Propane. *J. Catal.* **2012**, *296*, 120−131.
(43) Grzybowska-Swierkosz, B. Vanadia−Titania Catalysts for Oxidation of *o*-Xylene and Other Hydrocarbons. *Appl. Catal. A: Gen.* **1997**, *157*, 263−310.
(44) Wachs, I. E.; Weckhuysen, B. M. Structure and Reactivity of Surface Vanadium Oxide Species on Oxide Supports. *Appl. Catal. A: Gen.* **1997**, *157*, 67−90.
(45) Wachs, I. E. The Generality of Surface Vanadium Oxide Phases in Mixed Oxide Catalysts. *Appl. Catal. A: General* **2011**, *391*, 36−42.
(46) Weckhuysen, B. M.; Keller, D. E. Chemistry, Spectroscopy and the Role of Supported Vanadium Oxides in Heterogeneous Catalysis. *Catal. Today* **2003**, *78*, 25−46.

(47) Muylaert, I.; Van Der Voort, P. Supported Vanadium Oxide in Heterogeneous Catalysis: Elucidating the Structure-Activity Relationship with Spectroscopy. *Phys. Chem. Chem. Phys.* **2009**, *11*, 2826−2832.
(48) Launay, H.; Loridant, S.; Nguyen, D. L.; Volodin, A. M.; Dubois, J. L.; Millet, J. M. M. Vanadium Species in New Catalysts for the Selective Oxidation of Methane to Formaldehyde: Activation of the Catalytic Sites. *Catal. Today* **2007**, *128*, 176−182.
(49) Shvets, V. A.; Kazansky, V. B. Oxygen Anion-Radicals Adsorbed on Supported Oxide Catalysts Containing Ti, V and Mo Ions. *J. Catal.* **1972**, *25*, 123−130.
(50) Volodin, A. M.; Bolshov, V. A. ESR Study of Oxidation of a Partially Reduced V_2O_5/SiO_2 Catalyst by Molecules of O_2 and N_2O. *Kinet. Catal.* **1993**, *34*, 142−146.
(51) Avdeev, V. I.; Bedilo, A. F. Molecular Mechanism of Oxygen Isotopic Exchange over Supported Vanadium Oxide Catalyst VOx/TiO_2. *J. Phys. Chem. C* **2013**, *117* (6), 2879−2887.
(52) Avdeev, V. I.; Bedilo, A. F. Electronic Structure of Oxygen Radicals on the Surface of VOx/TiO_2 Catalysts and Their Role in Oxygen Isotopic Exchange. *J. Phys. Chem. C* **2013**, *117*, 14701−14709.
(53) Malykhin, S. E.; Volodin, A. M.; Bedilo, A. F.; Zhidomirov, G. M. Generation of O- Radical Anions on MgO Surface: Long-Distance Charge Separation or Homolytic Dissociation of Chemisorbed Water? *J. Phys. Chem. C* **2009**, *113*, 10350−10353.
(54) Volodin, A. M.; Malykhin, S. E.; Zhidomirov, G. M. O-Radical Anions on Oxide Catalysts: Formation, Properties, and Reactions. *Kinet. Catal.* **2011**, *52*, 605−619.
(55) Pakhomov, N. A.; Ivanova, A. S.; Bedilo, A. F.; Moroz, E. M.; Volodin, A. M. New Approach to Preparation and Investigation of Active Sites in Sulfated Zirconia Catalysts for Skeletal Isomerization of Alkanes. *Stud. Surf. Sci. Catal.* **2002**, *143*, 353−360.
(56) Stamires, D. N.; Turkevich, J. Electron Spin Resonance of Molecules Adsorbed on Synthetic Zeolites. *J. Am. Chem. Soc.* **1964**, *86*, 749−757.
(57) Nash, M. J.; Shough, A. M.; Fickel, D. W.; Doren, D. J.; Lobo, R. F. High-Temperature Dehydrogenation of Bronsted Acid Sites in Zeolites. *J. Am. Chem. Soc.* **2008**, *130*, 2460−2462.